ed to a thickness of 2 to 3 m as far as 30 km downwind. Pyroclastic flows extended more than 20 km, and some mudflows traveled as far as 120 km downstream. Approximately 5 km^3 of airborne tephra and 3 to 5 km^3 of pyroclastic and debris flows were produced (*6*).

After an apparent hiatus of approximately 5700 years, Glacier Peak again became active (Fig. 2). The resumption of eruptive behavior after thousands of years of dormancy underscores the difficulty of determining whether quiescent volcanoes are dormant or truly extinct. From 5500 to 5100 years ago, domes were emplaced near the summit of Glacier Peak and block and ash flows repeatedly swept down the flanks of the volcano. Valleys adjacent to the volcano were buried by at least 9 km^3 of debris. At the same time, mudflows and floods carried volcanic detritus at least 100 km down the Skagit River valley (*7*).

Apparently there followed a 2300-year interval of dormancy, during which streams and glaciers from the volcano cut valleys 100 to 300 m deep in the older volcanic valley fills. Around 2800 years ago, several mudflows traveled more than 20 km down the valley west of Glacier Peak. These may have been generated as a consequence of dome emplacement near the glaciated summit of the volcano, although no pyroclastic deposits of this age have been recognized.

Eruptions 1700 to 1800 years ago produced pyroclastic flows and mudflows which buried valleys on the east and west flanks of the volcano beneath as much as 100 m of debris. Mudflows and floods carried volcanic debris at least 100 km to the Skagit River delta. Several small towns in the lower Skagit River valley are built on volcanogenic sedimentary deposits of this age. Approximately 0.5 to 1.0 km^3 of new lithic material was ejected.

Sometime after 1800 years ago, a large mudflow containing hydrothermally altered volcanic rock traveled at least 30 km down the valley west of Glacier Peak. It is not known whether this flow was associated with a volcanic eruption, as other debris flows at Mount St. Helens (May 1980) and Mount Rainier (*8*) have been.

Many mudflows and some pyroclastic flows were produced in a complex series of events 1100 to 1000 years ago. Deposits of this age can be traced as much as 30 km downstream, and they locally buried valleys to depths of 80 to 100 m. About 0.10 to 0.25 km^3 of debris was ejected.

Between 1000 and 300 years ago, large floods and mudflows deposited debris 30 to 50 km down the valleys heading on the volcano. It is possible that small eruptions triggered the floods and mudflows, although no correlative pyroclastic deposits have been identified on the flanks of the volcano.

Early settlers and explorers did not record any eruptions of Glacier Peak. Nonetheless, Indian accounts suggest that Glacier Peak erupted sometime in the 18th century (*9*). These oral accounts are corroborated by the discovery of pumice and ash on moraines that are about 350 years old, indicating that the most recent eruption of Glacier Peak occurred in the 17th or 18th century.

The geological record shows that, during the past several thousand years, Glacier Peak has been one of the most active Cascade volcanoes. It erupted at least once in the past few centuries and many times since the end of the most recent ice age. If future eruptions at Glacier Peak resemble those of the past several thousand years, the chief hazards would be pyroclastic flows and superheated ash clouds near the volcano and mudflows and floods extending tens of kilometers. However, a sequence of events similar to that which occurred at Mount St. Helens in 1980, including the emplacement of a dome high in the glaciated cone and the concomitant eruption of a directed blast and large volumes of pumice and ash, is also possible. The recency and frequency of past volcanic events at Glacier Peak indicates that future monitoring is warranted.

JAMES E. BEGET*
Department of Geological Sciences,
University of Washington, Seattle 98105

References and Notes

1. S. C. Porter, *Quat. Res. (N.Y.)* **10**, 30 (1978).
2. S. L. Harris, *Fire and Ice* (Mountaineers–Pacific Search, Seattle, 1976).
3. R. W. Tabor and D. F. Crowder, *U.S. Geol. Surv. Prof. Pap. 604* (1969); D. R. Crandell, *U.S. Geol. Surv. Misc. Field Invest. Map MF—774* (1968); B. McKee, *Cascadia* (McGraw-Hill, New York, 1972); A. B. Ford, thesis, University of Washington, Seattle (1957).
4. Radiocarbon dates, stratigraphy, volume, and areal extent of deposits are summarized from an unpublished report completed for the Volcanic Hazards Project of the U.S. Geological Survey. Dates exceeding 300 years are radiocarbon years before present and are based on the Libby half-life (5568 ± 30 years) referenced to A.D. 1950. Dates under 300 years are based on tree ring counts.
5. J. A. Westgate and M. E. Evans, *Can. J. Earth Sci.* **15**, 1554 (1978); R. W. Lemke, M. R. Mudge, R. E. Wilcox, H. A. Powers, *U.S. Geol. Surv. Bull. 1395-H* (1975); D. R. Mullineaux, *U.S. Geol. Surv. Bull. 1326* (1974); R. Fryxell, *Science* **147**, 1288 (1965); D. R. Crandell, D. R. Mullineaux, R. D. Miller, M. Rubin, *U.S. Geol. Surv. Prof. Pap. 450-D* (1962).
6. J. E. Beget, in *Tephra Studies*, S. Self and R. S. J. Sparks, Eds. (Reidel, Dordrecht, Netherlands, 1981), pp. 449–457.
7. J. E. Beget, *Geol. Soc. Am. Abstr. Programs* **12**, 384 (1980); *ibid.* **11**, 68 (1979).
8. D. R. Crandell, *U.S. Geol. Surv. Prof. Pap. 677* (1969).
9. H. Majors, *Northwest Discov.* **1**, 109 (1980).
10. Partially supported by the Volcanic Hazards Projects of the U.S. Geological Survey and by grants from Sigma Xi and the Corporation Fund of the University.

* Present address: Geothermal Department, Chevron Resources Company, P.O. Box 3722, San Francisco, Calif. 94119.

16 June 1981; revised 7 December 1981

Kinetics of Delignification: A Molecular Approach

Abstract. *A treelike model has been proposed for the structure of lignin. Kinetics of delignification are formulated to account for the cleavage of linkages along the linear primary chains and at the cross-links. Experimental data obtained from isothermal delignification are used to verify this theory. Good agreement has been obtained in calculating the delignification curves. Activation energies are found to be 172 kilojoules per mole of cross-links and 132 kilojoules per mole of aryl ether bonds.*

Delignification is a major chemical process in the pulping of wood. The process has a long history, with a highly empirical kinetic description developed 40 years ago. Recently, I proposed a molecular model for lignin structure and a kinetic scheme associated with the delignification process (*1*). The model is broad enough to account for the linear and branched-chain structure of lignin; the kinetics are simple and flexible enough to allow for detailed curve fitting of experimental data. Experimental verification of this kinetic scheme is reported here.

The structural model used to describe lignin is the treelike model for branched polymers (*2–4*). Natural and insoluble lignins are regarded as a polymeric gel which coexists with the sol (soluble) fraction at any stage of delignification. The structure of lignin is described by units, linkages, and functionality defined as follows. (i) The basic unit is a phenylpropane (C_9) unit. Each unit contains one phenolic hydroxyl group, which may be free or bound (as aryl ether). (ii) Two C_9 units can be connected by only one linkage, regardless of the number of bonds between them. Thus in Fig. 1a, a linkage contains one bond. The linkages in Fig. 1, b and c, have two and three bonds, respectively. (iii) The units are linked monofunctionally and bifunction-

0036-8075/82/0312-1390$01.00/0

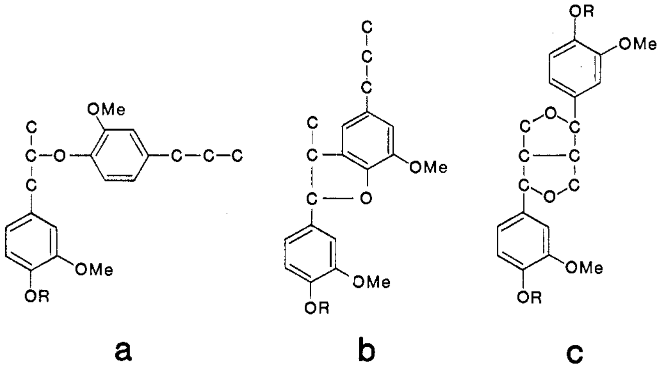

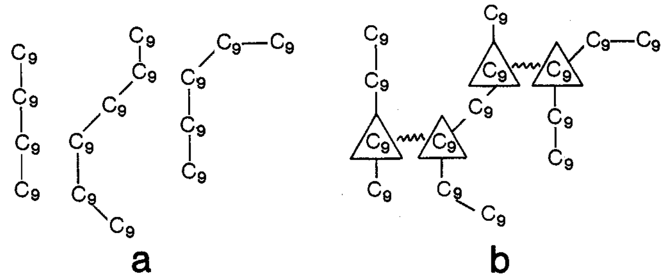

Fig. 1 (left). Interunit linkages between lignin units containing (a) one, (b) two, and (c) three chemical bonds. Fig. 2 (right). Primary chains (a) before and (b) after cross-linking.

ally to form linear (primary) chains, as shown in Fig. 2a. The "extent of reaction" in linear chains is denoted by p. (iv) Nonterminal units in two linear chains may be cross-linked to form a treelike polymer (*1*) as shown in Fig. 2b. A cross-linked unit (shown as a triangle) has a functionality of three. A pair of trifunctionally linked units form a cross-link (shown by zigzag lines in Fig. 2b) or a tetrafunctional branch point (*1–3*). The fraction of trifunctionally linked units is denoted by ρ.

Linear chains are assumed to have a most probable distribution, with a weight average degree of polymerization given by:

$$\bar{y}_w = (1 + p)/(1 - p) = 1 + \lambda \qquad (1)$$

These linear chains are then cross-linked to form lignin macromolecules, which become an insoluble gel at high conversion (*2, 3*).

In our model delignification is treated as degelation, or the reverse of gelation. In a batch process the total number of C_9 units is fixed. Degradation along the primary chains is kinetically expressed as

$$-\frac{dp}{dt} = k\,(p - p_c) \qquad (2)$$

Table 1. Rate constants calculated for the kraft pulping of spruce (*5*), $\lambda_0 = 27$, $\rho_0 = 0.1$. The tabulated numbers allow the evaluation of activation energies (E_a). With the six temperatures listed here I obtained $\ln k_2 = -20{,}700/T + 41.0$, $r^2 = 0.95$, $E_a = 172$ kJ/mole; and $\ln k = -15{,}900/T + 31.5$, $r^2 = 0.98$, $E_a = 132$ kJ/mole.

Temperature (K)	k_2 (min^{-1})	k (min^{-1})	r^2
403	0.00002	0.00036	0.93
423	0.00071	0.00178	0.99
443	0.00614	0.01842	0.98
448	0.00645	0.02258	0.98
453	0.00726	0.02178	0.99
458	0.00931	0.03259	0.98

where p_c is the critical value (gel point) at which all lignin molecules in a "digester" are made soluble when $t \rightarrow \infty$. The quantity $p - p_c$ represents the fraction of cleavable aryl ether bonds. As before (*1*), I use $p_c = 0.55$. This value is specific to the delignification of gymnosperms (softwood) by the kraft process.

Degradation also occurs at the cross-links. The kinetics of breaking the cross-links is given by

$$\frac{d\rho}{dt} = k_1\rho - k_2\,(1 - \rho)^2 \qquad (3)$$

The weight fraction of the gel, w_g, and that of the sol, w_s, are calculated from

$$1 - w_g = w_s = (1 - \rho)\,u + \rho u^2 \qquad (4)$$

where u is the extinction probability. The derivations and calculations are given in detail in (*1*).

Isothermal pulping data are usually expressed by plotting w_g against time t. Or, anticipating first-order behavior (*5*), the delignification is depicted as a plot of log w_g against t. To examine the general shape of the curve, or the trend in delignification, I calculated (*1*) the dependence of w_g on τ from Eqs. 2 to 4, where τ is a dimensionless time defined by

$$\tau = k_2 t \qquad (5)$$

The degradation of linear chains can also be expressed in terms of τ as

$$b\tau = kt \qquad (6)$$

The value of k_1 in Eq. 3 is not constant, but changes with the instantaneous average length of linear chains (*1*).

By estimating the three parameters λ_0, ρ_0, and b (where the subscript zero denotes the values at $t = 0$), w_g can be calculated at an assigned value of τ. This is the method adopted to calculate a theoretical delignification curve (*1*).

To verify this molecular approach, the calculation is reversed. That is, experimental values of w_g are used to calculate the corresponding values of τ. These τ values are then compared with the experimentally measured t values. Equation 5 suggests a linear relation between τ and t with slope k_2. A computer program is used to handle the calculation. The linearity of a plot of τ against t is checked by calculating the correlation coefficient r. The program then adjusts the three parameters to maximize r^2.

Using data obtained by Kleinert (*5*) at six temperatures, I found that the parameters which maximize r^2 are $\lambda_0 = 27$ and $\rho_0 = 0.1$. However, instead of the simple proportionality in Eq. 5, the form

$$\tau = k_2\,(t - t_0) \qquad (5a)$$

was obtained, where t_0 can be interpreted as the real zero time for the sample to reach the desired temperature. From k_2 and b, k can be calculated from Eq. 6. The calculated rate constants are shown in Table 1.

The calculated delignification curves at three temperatures are shown in Fig. 3, together with data obtained by Kleinert (*5*) in his isothermal delignification experiments. Three sets of data at 130°, 150°, and 175°C are not shown in Fig. 3. However, their fit is as good as that of the data which are shown; this is also evident in the high r^2 values in Table 1.

The molecular model describes the

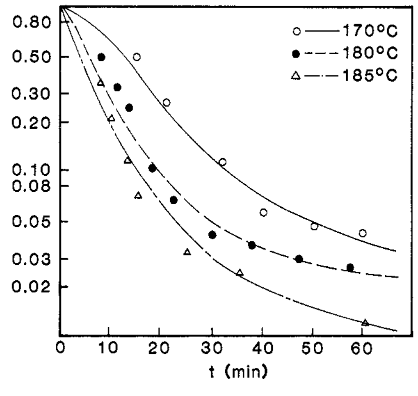

Fig. 3. Calculated kraft delignification curves and experimental data for spruce (*5*) at 170°, 180°, and 185°C.

entire delignification kinetic process (*5*). Furthermore, the activation energy obtained for the cleavable aryl ether bonds, 132 kJ/mole, is in good agreement with the value of 123 ± 9 kJ/mole obtained from model compound kinetics (*6*). The agreement value of the 134 kJ/mole (32 kcal/mole) obtained by the empirical power law technique (*5*) is considered fortuitous because this technique lacks a molecular basis (*1*). Values of k in Table 1 are of the same order of magnitude as those obtained for model dimers (*6*).

There is no experimental value to compare with the calculated activation energy for the cross-linking reaction. This reaction is also known as a recondensation in which the cross-links formed may no longer involve phenolic hydroxyl groups in the kraft medium (*1*).

I conclude that the treelike model can be used to elucidate the structure and reactions of lignin both qualitatively and quantitatively. Specifically, the model is capable of interpreting the following properties of lignin: (i) classification and identification of cleavable linkages, (ii) change of molecular weight averages and distribution of the lignin sol with delignification (*1*, *7*), and (iii) kinetics of delignification.

JOHNSON F. YAN
Weyerhaeuser Technology Center,
Weyerhaeuser Company,
Tacoma, Washington 98477

References

1. J. F. Yan, *Macromolecules* **14**, 1438 (1981).
2. P. J. Flory, *Principles of Polymer Chemistry* (Cornell Univ. Press., Ithaca, N.Y., 1953), chap. 9.
3. W. H. Stockmayer, *J. Chem. Phys.* **11**, 45 (1943).
4. K. Dusek, *Makromol. Chem. Suppl.* **2**, 35 (1979).
5. T. N. Kleinert, *Tappi* **49** (No. 2), 53 (1966).
6. S. Ljunggren, *Sven. Papperstidn.* **83**, 363 (1980).
7. J. F. Yan and D. C. Johnson, *J. Agric. Food Chem.* **28**, 850 (1980).

28 September 1981

Dating of a Fault by Electron Spin Resonance on Intrafault Materials

Abstract. *The total dose of natural radiation and the age were determined from paramagnetic defects in quartz grains at a fractured fault zone. Young age at the fault indicates that the accumulated defects in rocks were destroyed by high stress or high temperature at the time of the last fault movement, setting the clock time to zero. The technique was applied to quartz grains crushed by uniaxial compression in the laboratory to verify this interpretation.*

The time of formation or movement of an active fault is important for tracing the history of large earthquakes and assessing the safety of construction sites for nuclear power stations or large buildings from a geological point of view. Fault and fault movement have been studied extensively in geology and geography (*1*, *2*). Generally, faults are accompanied by fracture zones composed of the breccia and gouge called intrafault material. Fault movement has been dated by applying the potassium-argon method to an illite in intrafault materials (*3*) and by fission track dating of epidotes formed along the fault plane (*4*). We have developed a method of estimating the time of fault formation or last movement by dating quartz grains from intrafault materials by an electron spin resonance (ESR) method.

Electron spin resonance is useful for the study of natural radiation damage in geological materials (*5–7*) and for dating such biological materials (*8*) as shells, corals (*9*), and fossil bones and teeth (*10*). Its use for dating fault movement is based on the premise that the lattice defects produced by natural radiation in quartz grains are annihilated by high shearing stress and temperature rise around the fault plane at the time of fault formation or movement. It is assumed that the clock time was set to zero when the movement occurred. This is similar to the assumption made in thermoluminescence dating of ceramics that the firing of clays by ancient humans set the clock time to zero (*11*). Natural radiation after that time then produces additional lattice defects.

Quartz and feldspar were separated with a magnetic separator from intrafault gouge (clay) and breccia from the Atotsugawa fault, a typical active fault in central Japan (*12*). Fine grains 74 to 250 μm in diameter were sieved and immersed in HCl for 8 hours. Measurements were made at room temperature with an X-band ESR spectrometer (Japan Electron Optics FE) with 100-kHz field modulation. Artificial gamma irradiation was carried out with a ^{60}Co source.

Figure 1 shows an ESR derivative absorption spectrum of such grains taken from the intrafault material. A signal associated with radiation-induced de-

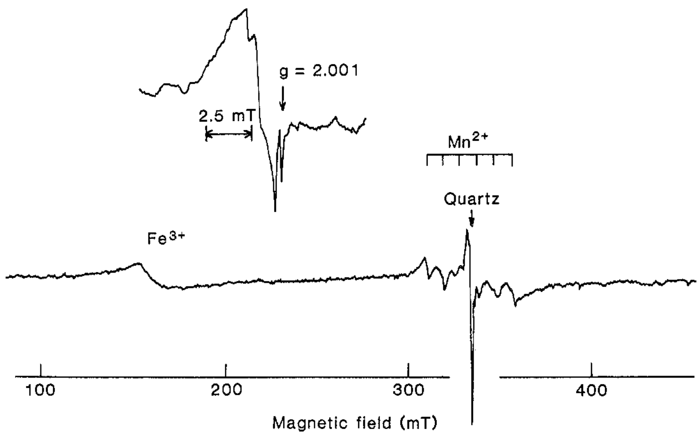

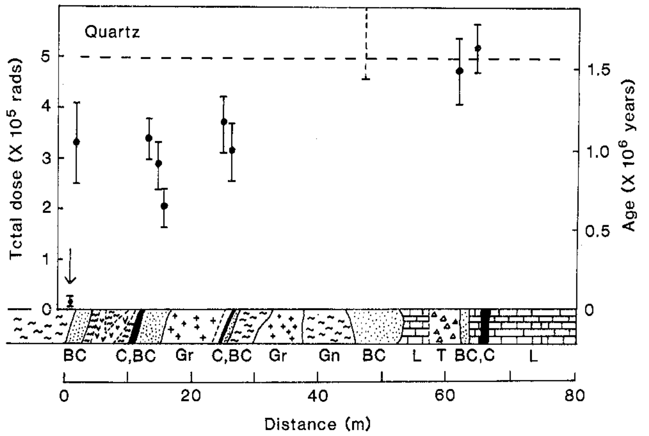

Fig. 1 (left). Electron spin resonance derivative absorption spectrum of quartz grains separated from gouge from Atotsugawa fault. An expanded spectrum of the signal associated with radiation damage in quartz is shown at the top. Fig. 2 (right). Total dose of natural radiation of quartz grains at several sites in the Atotsugawa fault zone. The smallest TD at the age of the fault zone is indicated by the arrow. The age based on the TD and an annual dose rate of 310 mrad is shown on the right ordinate. The abbreviations *BC*, *C*, *Gr*, *Gn*, *L*, and *T* indicate brecciated clay, clay, granite, gneiss, limestone, and talus, respectively.

0036-8075/82/0312-1392$01.00/0 Copyright © 1982 AAAS